[CANCER RESEARCH 63, 8122–8125, December 1, 2003]

Advances in Brief

A Multimodal Nanoparticle for Preoperative Magnetic Resonance Imaging and Intraoperative Optical Brain Tumor Delineation

Moritz F. Kircher, Umar Mahmood, Raymond S. King, Ralph Weissleder, and Lee Josephson

Center for Molecular Imaging Research, Massachusetts General Hospital and Harvard Medical School, Charlestown, Massachusetts

Abstract

The determination of brain tumor margins both during the presurgical planning phase and during surgical resection has long been a challenging task in the therapy of brain tumor patients. Using a model of gliosarcoma with stably green fluorescence protein-expressing 9L glioma cells, we explored a multimodal (near-infrared fluorescent and magnetic) nanoparticle as a preoperative magnetic resonance imaging contrast agent and intraoperative optical probe. Key features of nanoparticle metabolism, namely intracellular sequestration by microglia and the combined optical and magnetic properties of the probe, allowed delineation of brain tumors both by preoperative magnetic resonance imaging and by intraoperative optical imaging. This prototypical multimodal nanoparticle has unique properties that may allow radiologists and neurosurgeons to see the same probe in the same cells and may offer a new approach for obtaining tumor margins.

Introduction

The determination of tumor margins is so crucial to successful outcomes for brain tumor patients undergoing surgery that a wide variety of approaches have been explored in efforts to obtain a clearer identification of tumor margins. Intraoperative optical methods based either on the intrinsic properties of tissue or on the fluorescence of administered probes may assist the neurosurgeon but cannot be used to relate preoperative radiological images to the visual presentation of pathology during surgery (1–3). MRI[1] equipment can be adapted for use in the operating room (4), but instruments are expensive and available in only a few medical centers. Contrast enhanced MRI with gadolinium chelates suffer issues of timing (5), dose (6), and surgically induced contrast enhancement (7).

We hypothesized that a multimodal nanoparticle contrast agent consisting of an optically detectable NIRF fluorochrome conjugated to a MRI-detectable iron oxide core might offer a novel approach to the surgical resection of brain tumors. Magnetic nanoparticles have been evaluated preclinically and clinically for their ability to aid in brain tumor visualization by MRI (8–10). We found that the multimodal nanoparticle probe termed Cy5.5-CLIO permitted the preoperative visualization of brain tumors by serving as an MRI contrast agent and afforded an intraoperative discrimination of tumors from brain tissue because of its near-IR fluorescence. The ability to track the same probe by both preoperative MR and intraoperative optical imaging offers a new approach to visualization and accurate resection of tumors.

Materials and Methods

Synthesis of Cy5.5-CLIO. The NH_2-CLIO nanoparticle (11, 12) at 0.2 ml at 10 mg Fe/ml in 0.02 M citrate (pH 8) was added to a tube of Cy5.5 (Amersham-Pharmacia) at room temperature for 2 h, with subsequent incubation at 4°C overnight. Unreacted Cy5.5 was removed by gel filtration [Sephadex G-25 in 0.02 M citrate, 0.15 M NaCl (pH 8)]. The number of dyes/crystal was obtained from the absorbance at 675 nm using an extinction coefficient of 250,000 $M^{-1}cm^{-1}$ for Cy5.5. Iron concentration was assayed as previously described (11), and the concentration of nanoparticles obtained by assuming 2064 iron atoms/crystal (13). The nanoparticle, Cy5.5-CLIO, was 32 nm using the volume estimation of laser light scattering (Malvern Instruments) and had an average of 1 Cy5.5 dye/crystal.

Animal Model. A 9L rat gliosarcoma cell line stably transfected to express GFP (14) was cultured at 37°C in a humidified 5% CO_2 atmosphere in DMEM supplemented with 10% fetal bovine serum, 1% penicillin/streptomycin, and 500 μg/ml Geniticin G418 (all products from Cellgro, Herndon, VA). The medium was changed every 3 days, and cells were passaged once/week (1:10 split ratio).

Eight Fisher 344 rats (Charles River Laboratories, Wilmington, MA), 200–250 g, were anesthetized with ketamine/xylazine (i.p., 65/10 mg/kg) and immobilized in a stereotactic frame. A linear skin incision was made over the bregma, and a 1-mm diameter burrhole was drilled into the skull 3 mm posterior and 3 mm lateral to the bregma. A 10-μl gas-tight syringe (Hamilton, Reno, NV) was then used to inject 5 μl of the 9L-GFP-cell suspension (10^6 cells in HBSS) in the striatum at a depth of 3 mm from the dural surface. The injection was done slowly over 5 min, and the needle was withdrawn over another 10 min. The burrhole was occluded with bone wax (Ethicon, Sommerville, NJ) to prevent leakage of cerebrospinal fluid, and the skin was closed with nonmagnetic sutures. MRI of rats was performed 10–14 days after tumor inoculation, when the tumors had reached diameters of ~2–5 mm, 24 h after i.v. injection of 15 mg Fe/kg Cy5.5-CLIO.

MRI. Animals were injected with 15 mg/kg body weight Cy5.5-CLIO via tail vein injection. After 24 h, MRI was performed at 4.7 T (Bruker Instruments, Billerica, MA) equipped with a 30 gauss/cm gradient set and a 37-mm diameter birdcage coil resonating at 200 MHz. Multiple slice multiple echo Proton-density/T2-weighted (TR/TE 15, 30, 45, 60/2000) spin echo sequences were obtained using 2 NEX, a 256 × 256 matrix, a 3.0-cm field of view (resulting in an in-plane resolution of 117 μm), a slice thickness of 1 mm and a total imaging time of 17 min. For MRI-histology correlation, rats were sacrificed (pentobarbital, i.p. 200 mg/kg), perfused with 250 ml of PBS, and brains were stained (H&E and DAB-amplified Prussian Blue).

Optical Imaging. Twenty-four h after i.v. injection of 15 mg/kg body weight Cy5.5-CLIO, a craniotomy was performed to operatively expose the tumor and surrounding tissue. Noninvasive optical imaging was performed using a custom built surface reflectance imaging system (Siemens Medical Systems, Erlangen, Germany) based on a multichannel imaging system design (15). The system is capable of near simultaneous data acquisition in four channels, including a broad spectrum visible white light similar as seen by the unaided eye, an excitation/emission filter set for GFP imaging, and a filter set for Cy5.5 imaging. Images were acquired with an exposure time of 400, 500, and 200 ms for the GFP, Cy5.5, and white light channels, respectively.

Histology. The distribution of tumor in the brain was determined by GFP fluorescence and Cy5.5 fluorescence 24 h after i.v. injection of 15 mg/kg body weight Cy5.5-CLIO. Tumors were cryosectioned, and fluorescence micros-

Received 8/5/03; revised 9/23/03; accepted 9/29/03.

Grant support: NIH Grant P50 CA86355. M. F. K. was supported by the German Research Foundation (Deutsche Forschungsgemeinschaft). R. S. K. was supported by a NIH T32 Training Grant.

The costs of publication of this article were defrayed in part by the payment of page charges. This article must therefore be hereby marked *advertisement* in accordance with 18 U.S.C. Section 1734 solely to indicate this fact.

Requests for reprints: Lee Josephson, Center for Molecular Imaging Research, Massachusetts General Hospital, 13th Street, Building 149, Room 5406, Charlestown, MA 02129. Phone: (617) 726-6478; Fax: (617) 726-5708; E-mail: josephso@helix.mgh.harvard.edu.

[1] The abbreviations used are: MRI, magnetic resonance imaging; CLIO, cross-linked iron oxide nanoparticle; NIRF, near-infrared fluorescence; IR, infrared; GFP, green fluorescence protein; DAB, 3,3′-diaminobenzidine.

copy of GFP and Cy5.5 fluorescence was performed on air-dried sections using an inverted epifluorescence microscope (Axiovert 100; Zeiss, Thornwood, NY). A cooled charge-coupled device camera (Sensys; Photometrics, Tucson, AZ) was used for image capture. Sections were subsequently stained with H&E and DAB-amplified Prussian Blue and examined with bright light microscopy.

Slices were also examined by laser-scanning confocal microscopy using a Zeiss LSM 5 Pascal. Glial cells were identified immunohistochemically using a primary monoclonal mouse-antirat antibody against CD11b (Serotec, Raleigh, NC) and a secondary rhodamine-labeled rabbit antimouse antibody (Jackson Immnunoresearch Laboratories, West Grove, PA). The fluorescence from GFP (tumor), Cy5.5 (nanoparticle), and the rhodamine (glia cells and macrophages) were obtained by selecting appropriate excitation and emission settings.

Accuracy of Determining Tumor Extent via Cy5.5 Fluorescence. Five brain tumors were cryosectioned into four to eight slices each, resulting in 25 slices (20-μm slice thickness with an interleave of 500 μm) and digital images of tumors and surrounding brain tissue captured using an inverted fluorescence microscope equipped with a charge-coupled device camera (Zeiss Axiovert 100). Regions of interest were placed on digitized images around borders of the tumor as defined by GFP and Cy5.5 fluorescence using CMIR-Image [developed in Interactive Data Language (Research Systems Inc, Boulder, CO)]. The area of each region of interest on each slice was computed, and the values of Cy5.5 and GFP-positive areas plotted with a linear regression analysis using Microsoft Excel.

Results

To demonstrate the ability of Cy5.5-CLIO nanoparticles to act as a contrast agent for preoperative brain tumor imaging, we performed MRI on brain tumor bearing rats. Fig. 1 shows a representative example of proton density-weighted (Fig. 1*A*) and T2-weighted images (Fig. 1*B*) after the administration of Cy5.5-CLIO. The hypointense tumor relative to the surrounding tissue on T2-weighted images (Fig. 1*B*) is indicative of nanoparticle accumulation, which causes reduction in signal intensity with T2-weighted spin echo pulse sequences. Reduction in signal intensity on T2-weighted but not proton density-weighted images is characteristic of monodisperse superparamagnetic iron oxide nanoparticles and not seen with larger magnetic particles or gadolinium chelates (16).

Subsequently, brains were cryosectioned coronally, with a slice orientation corresponding to that of the MRI, and histology was performed. There was high congruency between the signal reduction obtained on MRIs and tumor as determined by H&E staining (Fig. 1*C*). DAB-amplified Prussian blue stain (Fig. 1*D*) demonstrated the accumulation of iron in the tumor because staining was negative in uninjected animals (data not shown). The distribution of Cy5.5-CLIO in tumors was also determined by near-IR fluorescence, as described below.

We next examined whether Cy5.5-CLIO could be used to delineate brain tumors in a model intraoperative setting. Fig. 2 shows images of a rat after craniotomy and exposition of the tumor in the white light channel (Fig. 2*A*), in the GFP channel serving as the gold standard for delineation of true tumor extent (Fig. 2*B*), and in the Cy5.5 channel (Fig. 2*C*). Even with exposure times as short as 500 milliseconds, ample Cy5.5 fluorescence was obtained (Fig. 2*C*) to clearly visualize the tumor, as indicated by the correlation with the tumor extent as determined by GFP fluorescence (Fig. 2*B*). The relationship between tumor and Cy5.5 fluorescence was additionally examined by histology, using epifluorescence microscopy as shown in Fig. 2*F*. H&E staining (Fig. 2*D*) was compared with GFP fluorescence (Fig. 2*E*) and Cy5.5 fluorescence (Fig. 2*F*). To compare the accuracy of tumor margin delineation by Cy5.5-CLIO uptake with tumor margin delineation by GFP fluorescence, region of interest analysis of Cy5.5 and GFP-positive areas on 25 slices from five brain tumors was performed (see "Materials and Methods"). The areas obtained from these regions of interest were fitted with a linear regression analysis for all 25 slices as shown in Fig. 3. The data showed an excellent fit to a linear equation with a slope of 1.013, an intercept of 0.820 mm^2 and a R^2 of 0.996. The slightly higher estimate of tumor volumes obtained with Cy5.5 is caused by the uptake of Cy5.5-CLIO by microglia, as described below.

To determine the cellular distribution of Cy5.5-CLIO, we performed triple-channel laser scanning confocal microscopy. Fig. 4 compares the distribution of Cy5.5-CLIO [Cy5.5 channel (Fig. 4*A*)] with the distribution of tumor cells [GFP channel (Fig. 4*B*)] and microglia and macrophages [CD11b immunohistochemistry using the rhodamine channel

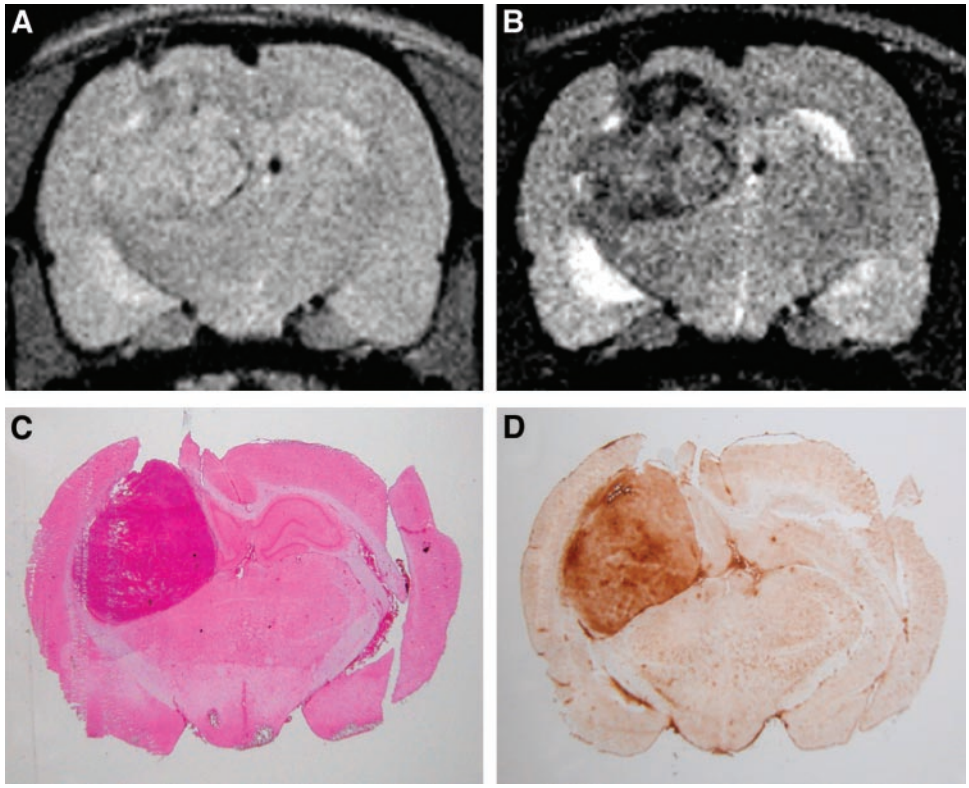

Fig. 1. Cy5.5-CLIO nanoparticle as a preoperative MRI contrast agent. Proton density and T2-weighted images are shown in *A* and *B*, respectively. Tumor uptake of iron is evident on T2-weighted images as regions of low signal intensity, whereas tumor is isointense to surrounding tissue using proton density images. *C*, H&E staining of histological section corresponding to MRI slices in *A* and *B*. *D*, DAB-amplified Prussian Blue staining of histological section corresponding to MRI slices in *A* and *B*.

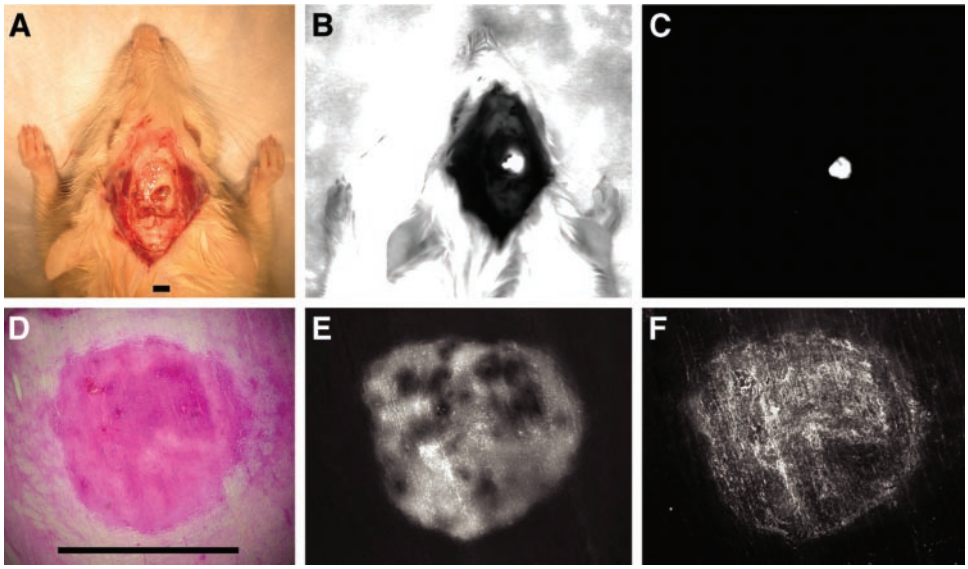

Fig. 2. Delineation of a GFP-expressing 9L glioma tumor by optical imaging in an intraoperative setting. Craniotomy was performed on a Fischer 344 rat bearing a 3-mm diameter 9L glioma tumor. The brain tissue overlying the tumor was removed and optical imaging performed. White light image (*A*), GFP channel (*B*), and Cy5.5-channel (*C*). *D–F*, histological processing and microscopy of the tumor shown in *A–C*. *D*, H&E stain; *E*, GFP channel; *F*, Cy5.5 channel (20-μm sections, original magnification, ×2.5). *Scale bar* = 5 mm.

(Fig. 4*C*)]. Cy5.5-CLIO was strongly associated with CD11b-positive cells (Fig. 4*D*) and much less with GFP-positive cells (Fig. 4*E*).

We next examined the tumor border as defined by tumor cells (GFP channel, Fig. 4*F*) and by microglia (CD11b staining, Fig. 4*G*) with confocal microscopy. As the overlay Fig. 4*H* shows, the presence of microglia exhibits high congruency with GFP fluorescence at the tumor-brain interface. Microglia consistently extended slightly beyond the tumor border as defined by GFP fluorescence (Fig. 4*H*), consistent with the higher estimation of tumor area by Cy5.5 fluorescence as described in Fig. 3.

Discussion

We synthesized Cy5.5-CLIO, a long circulating iron oxide nanoparticle with a NIRF dye attached to a coating of cross-linked dextran, and investigated its use as a combined preoperative magnetic resonance contrast agent and intraoperative optical probe. Magnetic nanoparticles (10–100 nm) have long blood half-lives because they are too large to undergo renal elimination and too small to be easily recognized by phagocytes. They are eventually internalized, predominantly by cells of the reticuloendothelial system, and their superparamagnetic iron is dissolved and joins normal iron pools (17). In contrast, low molecular weight gadolinium chelates accumulate in the extracellular space where blood brain barrier breakdown has occurred. They undergo both rapid diffusion through the interstitium and renal elimination and therefore have the limitation of providing a time-dependent image of tumor margins. In response to these issues, long circulating magnetic nanoparticles have been investigated as magnetic resonance contrast agents, with the hope of providing better delineation of brain tumors (8, 9). The basic features of nanoparticle metabolism (internalization, storage, dissolution of the iron oxide) suggest that Cy5.5-CLIO will be localized inside the same cells during preoperative and intraoperative imaging procedures. A coinjection of a magnetic resonance contrast agent such as Gd-diethylenetriaminepentaacetic acid and optical probe such as indocyanine green (18) would not seem to offer the advantages of Cy5.5-CLIO for comparison of preoperative and intraoperative anatomy. Gd-chelates do not bind plasma proteins and undergo rapid renal elimination, whereas organic anions such as indocyanine green bind plasma proteins and undergo hepatobiliary elimination (5, 19). These compounds differ in their physical and biological properties and would be expected to have different biodistributions.

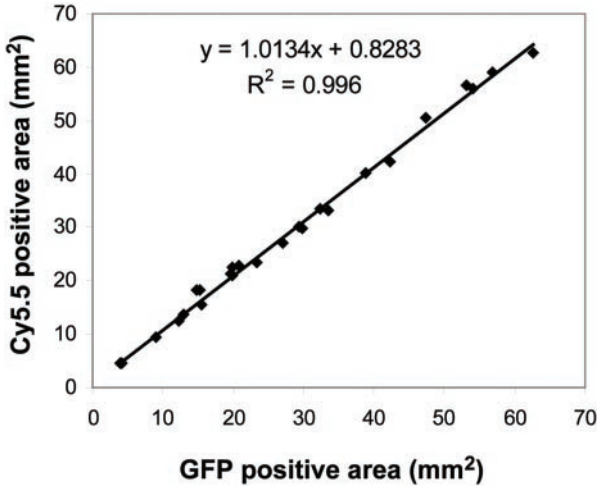

Fig. 3. Accuracy of Cy5.5 fluorescence in determining true tumor extent as defined by the gold standard GFP fluorescence. Five brain tumors were sliced in 4–8 slices each (25 slices total), and Cy5.5 and GFP-positive areas on slices were determined by region of interest analysis.

The attachment of the NIRF fluorochrome Cy5.5 to the NH_2-CLIO nanoparticle afforded several key advantages over a nonfluorescent nanoparticles or the use of non-IR fluorochromes. First, the NIRF signal from Cy5.5-CLIO was sufficiently strong that acquisition times as short as 500 ms provided easy identification of the tumor in a model intraoperative setting (Fig. 2*C*). Second, by using near-IR fluorescence, tissue autofluorescence was minimized because near-IR fluorescent fluorochromes have not been reported in brain, as illustrated in NIRF micrograph of brain tissue surrounding tumor in Fig. 2*C*. Third, near-IR fluorescence permitted the visualization of probes such as Cy5.5-CLIO through several millimeters of overlaying tissue, *i.e.*, before complete dissection of the tumor has been accomplished (20). Fourth, the NIRF obtained from our optical/magnetic nanoparticle was visualized with simple, low cost instrumentation, a version of which might easily be adapted to an operating room setting for human patients.

The correspondence between preoperative and intraoperative tumor coordinates is a significant challenge in surgery and one that the combined magnetic and optical properties of Cy5.5-CLIO can be used to overcome. However, a second problem in tumor resection is the often poorly defined tumor margins because of finger-like projections of tumor cells from the tumor or tumor cells that have migrated and

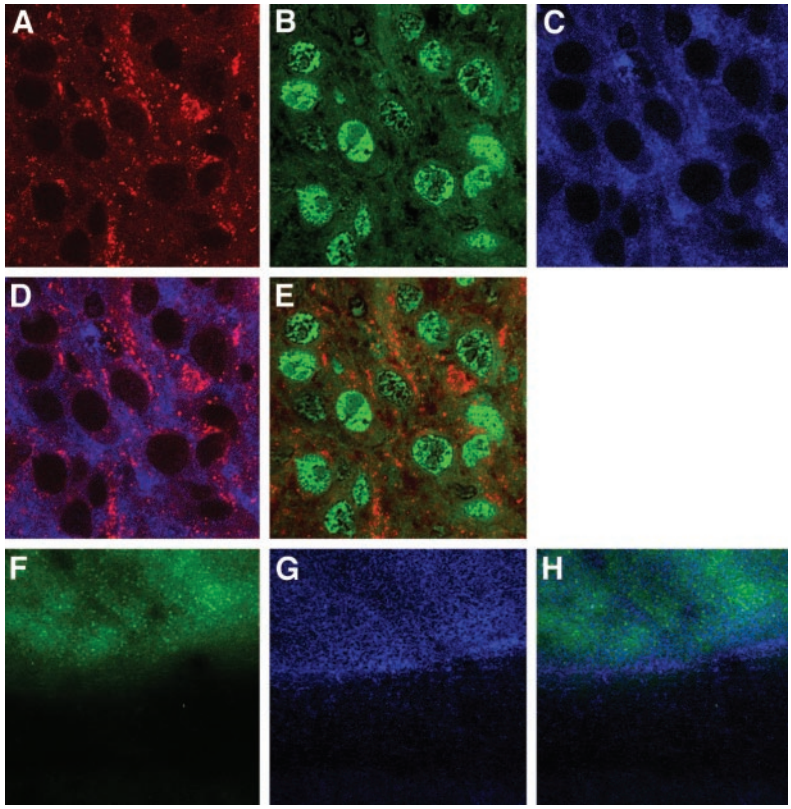

Fig. 4. Cell type internalizing Cy5.5-CLIO as determined by laser scanning confocal microscopy. *A–E*, area from tumor center, original magnification, ×200. *A*, distribution of Cy5.5-CLIO in Cy5.5 channel; *B*, GFP channel; *C*, anti-CD11b staining for microglia and macrophages in rhodamine channel; *D*, overlay of *A* and *C*; *E*, overlay of *A* and *B*. Cy5.5-CLIO is internalized predominantly by microglial cells and infiltrating macrophages. *F–H*, area from tumor-brain interface, original magnification, ×10. *F*, tumor border in GFP channel; *G*, tumor border in rhodamine channel (CD11b); *H*, overlay of *F* and *G*. Cells positive for CD11b extend slightly beyond the border of GFP fluorescence.

are not continuous with the tumor itself. The sensitivity of the method will depend not only on the amount and pattern of agent uptake by tumors but also on the detection limit of the NIRF-detecting instrumentation used. Additional research with multimodal nanoparticles is needed to address issues of tumor margin pathology, agent accumulation, and instrumentation in greater detail.

In conclusion, a multimodal magneto/optical nanoparticle offers a unique method for comparing the visual presentation of brain tumors during surgery with the multislice topographical capability of preoperative MRI. Our results indicate the feasibility of this approach using nanoparticles that are similar to those used clinically, which can be synthesized simply and which provide a strong NIRF signal enabling real-time imaging. The method can use existing MRI and simple NIRF/optical instrumentation and therefore can be cost effective. Key features of nanoparticles metabolism, namely intracellular sequestration and slow degradation, together with the combined optical and magnetic properties of Cy5.5-CLIO, may allow radiologists and neurosurgeons for the first time to see the same probe in the same cells. This may increase the precision of surgical resection and improve the outlook for many brain cancer patients.

References

1. Lin, W. C., Toms, S. A., Johnson, M., Jansen, E. D., and Mahadevan-Jansen, A. *In vivo* brain tumor demarcation using optical spectroscopy. Photochem. Photobiol., *73:* 396–402, 2001.
2. Eggert, H. R., and Blazek, V. Optical properties of human brain tissue, meninges, and brain tumors in the spectral range of 200 to 900 nm. Neurosurgery, *21:* 459–464, 1987.
3. Stummer, W., Stocker, S., Wagner, S., Stepp, H., Fritsch, C., Goetz, C., Goetz, A. E., Kiefmann, R., and Reulen, H. J. Intraoperative detection of malignant gliomas by 5-aminolevulinic acid-induced porphyrin fluorescence. Neurosurgery, *42:* 518–525; discussion 525–516, 1998.
4. Schulder, M., and Carmel, P. W. Intraoperative magnetic resonance imaging: impact on brain tumor surgery. Cancer Control, *10:* 115–124, 2003.
5. Ludemann, L., Hamm, B., and Zimmer, C. Pharmacokinetic analysis of glioma compartments with dynamic Gd-DTPA-enhanced magnetic resonance imaging. Magn. Reson. Imaging, *18:* 1201–1214, 2000.
6. Knauth, M., Wirtz, C. R., Aras, N., and Sartor, K. Low-field interventional MRI in neurosurgery: finding the right dose of contrast medium. Neuroradiology, *43:* 254–258, 2001.
7. Knauth, M., Aras, N., Wirtz, C. R., Dorfler, A., Engelhorn, T., and Sartor, K. Surgically induced intracranial contrast enhancement: potential source of diagnostic error in intraoperative MR imaging. AJNR Am. J. Neuroradiol., *20:* 1547–1553, 1999.
8. Fleige, G., Nolte, C., Synowitz, M., Seeberger, F., Kettenmann, H., and Zimmer, C. Magnetic labeling of activated microglia in experimental gliomas. Neoplasia, *3:* 489–499, 2001.
9. Enochs, W. S., Harsh, G., Hochberg, F., and Weissleder, R. Improved delineation of human brain tumors on MR images using a long-circulating, superparamagnetic iron oxide agent. J. Magn. Reson. Imaging, *9:* 228–232, 1999.
10. Knauth, M., Egelhof, T., Roth, S. U., Wirtz, C. R., and Sartor, K. Monocrystalline iron oxide nanoparticles: possible solution to the problem of surgically induced intracranial contrast enhancement in intraoperative MR imaging. AJNR Am J Neuroradiol., *22:* 99–102, 2001.
11. Josephson, L., Tung, C. H., Moore, A., and Weissleder, R. High-efficiency intracellular magnetic labeling with novel superparamagnetic-Tat peptide conjugates. Bioconjug. Chem., *10:* 186–191, 1999.
12. Josephson, L., Perez, J. M., and Weissleder, R. Magnetic nanosensors for the detection of oligonucleotide sequences. Angew. Chem. Int. Ed. Engl., *40:* 3204–3206, 2001.
13. Shen, T., Weissleder, R., Papisov, M., Bogdanov, A., Jr., and Brady, T. J. Monocrystalline iron oxide nanocompounds (MION): physicochemical properties. Magn. Reson. Med., *29:* 599–604, 1993.
14. Moore, A., Marecos, E., Simonova, M., Weissleder, R., and Bogdanov, A., Jr. Novel gliosarcoma cell line expressing green fluorescent protein: a model for quantitative assessment of angiogenesis. Microvasc. Res., *56:* 145–153, 1998.
15. Mahmood, U., Tung, C. H., Tang, Y., and Weissleder, R. Feasibility of *in vivo* multichannel optical imaging of gene expression: experimental study in mice. Radiology, *224:* 446–451, 2002.
16. Rogers, J., Lewis, J., and Josephson, L. Use of AMI-227 as an oral MR contrast agent. Magn. Reson. Med., *12:* 631–639, 1994.
17. Weissleder, R., Stark, D. D., Engelstad, B. L., Bacon, B. R., Compton, C. C., White, D. L., Jacobs, P., and Lewis, J. Superparamagnetic iron oxide: pharmacokinetics and toxicity. AJR Am. J. Roentgenol., *152:* 167–173, 1989.
18. Ntziachristos, V., Yodh, A. G., Schnall, M., and Chance, B. Concurrent MRI and diffuse optical tomography of breast after indocyanine green enhancement. Proc. Natl. Acad. Sci. USA, *97:* 2767–2772, 2000.
19. Thiessen, J. J., Rappaport, P. L., and Eppel, J. G. Indocyanine green pharmacokinetics in the rabbit. Can. J. Physiol. Pharmacol., *62:* 1078–1085, 1984.
20. Weissleder, R. and Ntziachristos, V. Shedding light onto live molecular targets. Nat. Med., *9:* 123–128, 2003.